# Theoretical Characterization of a Typical Hole/Exciton-Blocking Material Bathocuproine and Its Analogues

**Hongze Gao,[†] Chunsheng Qin,[‡] Houyu Zhang,[†] Shuixing Wu,[‡] Zhong-Min Su,*[,†,‡] and Yue Wang*[,†]**

*State Key Laboratory of Supramolecular Structure and Materials, Jilin University, Changchun 130012, Jilin, People's Republic of China, and Institute of Functional Material Chemistry, Faculty of Chemistry, Northeast Normal University, Changchun 130024, Jilin, People's Republic of China*

*Received: May 15, 2008; Revised Manuscript Received: June 30, 2008*

The structural, electronic, and carrier transport properties of bathocuproine (**BCP**), which is a typical hole/exciton-blocking material applied in organic light-emitting diodes (OLEDs), have been investigated based on density functional theory (DFT) and ab initio HF method. The detail characterizations of frontier electronic structure and lowest-energy optical transitions have been studied by means of time-dependent density functional theory (TD-DFT). Five **BCP** analogues, *o*-phenanthroline (**1**), 2,9-dimethyl-1,10-phenanthroline (**2**), 2,9-diphenyl-1,10-phenanthroline (**3**), 4,7-diphenyl-1,10-phenanthroline (**4**), and 2,9-bis(trifluoromethyl)-1,10-phenanthroline (**5**) have also been studied in order to select more suitable candidates of efficient hole-blocking materials. The calculated results showed that rigid planar structures, conjugate degrees, and substitute groups play crucial roles in the hole/exciton-blocking and electron-transport properties of these materials. The calculated geometries, ionization energies (IP), and energy gap between the singlet ground state and triplet excited state ($E_{T1}$) were well in agreement with the experimental results. On the basis of the incoherent transport model, the calculated electron mobility of **BCP** is $1.79 \times 10^{-2}$ cm$^2$/(V s), which is comparable to experimental results of $1.1 \times 10^{-3}$ cm$^2$/(V s). The electron mobilities for compounds **1**, **4**, and **5** are $3.45 \times 10^{-2}$, $2.90 \times 10^{-2}$, and $1.40 \times 10^{-2}$ cm$^2$/(V s), respectively. The calculated results indicated that compounds **1**, **4**, and **5** may be more effective hole/exciton-blocking materials than **BCP**.

## Introduction

In the last two decades, a great deal of effort has been invested in the studies of organic electroluminescent (EL) materials and devices.[1,2] It is well-known that most of organic EL materials are in favor of the injection and transport of holes rather than electrons; therefore, the recombinations between electrons and holes generally occur near the cathode, which could lead to the quenching of the excitons produced. To achieve highly efficient organic electroluminescence, it is essential to confine the excitons within the emitting layer and prevent the excitons and holes from approaching the cathode. Therefore, a hole/exciton-blocking layer (HBL) is often introduced between the emitting layer and the electron-transport layer in some organic electroluminescent diodes (OLEDs) (Figure 1). The hole/exciton-blocking layer plays a dual role in blocking holes to move toward the cathode and transporting the electrons into the emitting layer.

The efficient hole/exciton-blocking materials must possess the following three key characteristics: a wide energy band gap (singlet and triplet states, $E_{T1}$), a deep HOMO energy level (i.e., a high ionization energy, IP), and the LUMO energy level matching the electron-transport layer (ETL).[3] Besides those electronic properties, the material should have high intrinsic electron mobility. So far, the valuable hole/exciton-blocking materials are still very rare. It is necessary to explore a way to design and synthesize efficient hole/exciton-blocking materials.

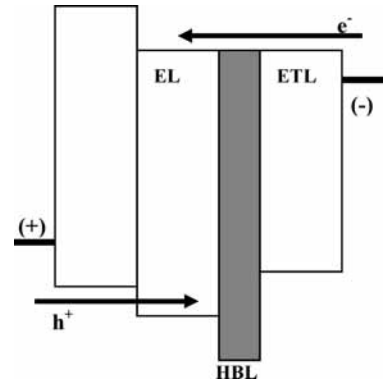


**Figure 1.** Schematic energy level diagram of an organic electroluminescent device in which a hole/exciton-blocking layer (HBL) is inserted between an emitting layer (EL) and an electron-transport layer (ETL). The arrows indictate the transport directions of the hole and electron along the HOMO and LUMO energy levels.

Bathocuproine (**BCP**) is currently widely used as an electron-transporting and hole/exciton-blocking material and has played an important role in the highly efficient OLEDs based on phosphorescent emitters such as iridium and platinum complexes.[3,4] Although some experimental works have focused on how the **BCP** layer determines the performance of the OLEDs,[5,6] it is still necessary to perform systematic theoretical studies of the relationship between the molecular structure and the hole/exciton-blocking ability of **BCP**. This will be a benefit to understanding the basic physical and chemical characteristics of **BCP**. From a molecular design point of view, it is possible to achieve better performance by appropriate molecular modi-

* To whom correspondence should be addressed. E-mail: zmsu@nenu.edu.cn (Z.M.S.); yuewang@jlu.edu.cn (Y.W.).
† Jilin University.
‡ Northeast Normal University.

10.1021/jp804308e CCC: $40.75 
Published on Web 08/27/2008

fications based on the **BCP** molecule. Therefore, the theoretical calculation of the **BCP**'s analogue molecules may give us some useful information for the design and synthesis of efficient hole/exciton-blocking materials. In this contribution, we report the theoretical studies of **BCP** and its analogue molecules.

## Theoretical Methodology and Computational Methods

To describe the charge-transport properties of **BCP**, the incoherent hopping model[7] was employed in which charge can transfer only between neighboring molecules. Each hopping step has been considered as a nonadiabatic electron-transfer reaction involving a self-exchange charge from a charged molecule to an adjacent neutral one. The rate of charge transfer between neighboring molecules, $k$, can be expressed by the standard Marcus equation[8] in terms of the reorganization energy $\lambda$, the transfer integral $\beta$, and the temperature $T$ as

$$k = \frac{4\pi^2}{h}\frac{1}{\sqrt{4\pi\lambda k_B T}}\beta^2 \exp\left(-\frac{\lambda}{4k_B T}\right) \quad (1)$$

where $h$ and $k_B$ are the Planck and Boltzmann constants. For a fixed temperature, the large transfer rate can be attributed to the maximal transfer integral and the minimal reorganization energy. The drift mobility of hopping, $\mu$, can be evaluated from the Einstein relation

$$\mu = \frac{e}{k_B T}D \quad (2)$$

where $e$ is the electronic charge and $D$ is the diffusion coefficient, which is related to the charge-transfer rate $k$ as summing over all possible hops. The diffusion coefficient can be approximately evaluated as[9]

$$D = \frac{1}{2n}\sum_i d_i^2 k_i P_i \quad (3)$$

where $n = 3$ is the dimensionality, $k_i$ is the hopping rate due to the charge carrier to the $i$th neighbor, $d_i$ is the distance to neighbor $i$, and $P_i$ is the relative probability for charge carrier to a particular $i$th neighbor

$$P_i = k_i / \sum_i k_i \quad (4)$$

Using eqs 1−4, the carrier mobility can be calculated. However, what is still lacking is how to obtain the intermolecular transfer integral $\beta$ and reorganization energy $\lambda$. The transfer integral characterizes the strength of electronic coupling between the two adjacent molecules. The charge-transfer integral can be obtained either by an indirect method (Koopmans's theorem at the Hartree−Fock mean-field level)[10] or by the direct dimer Hamiltonian evaluation method.[9d,e,11] In the former case, Valeev et al. cautioned recently that when the dimer is not cofacial, the site energy correction should be taken into account due to the crystal environment.[12] The charge-transfer integrals for electron transport could be obtained from the direct method and can be written as:

$$\beta = \langle \phi_{LUMO}^{0,site1} | F | \phi_{LUMO}^{0,site2} \rangle \quad (5)$$

where $\phi_{LUMO}^{0,site1}$ and $\phi_{LUMO}^{0,site2}$ represent the LUMOs of isolated molecules 1 and 2, respectively, and $F$ is the Fock operator for the dimer with a density matrix from the noninteracting dimer of $F = SC\varepsilon C^{-1}$, where $S$ is the intermolecular overlap matrix and $C$ and $\varepsilon$ are the molecular orbital coefficients and energies from one-step diagonalization without iteration.

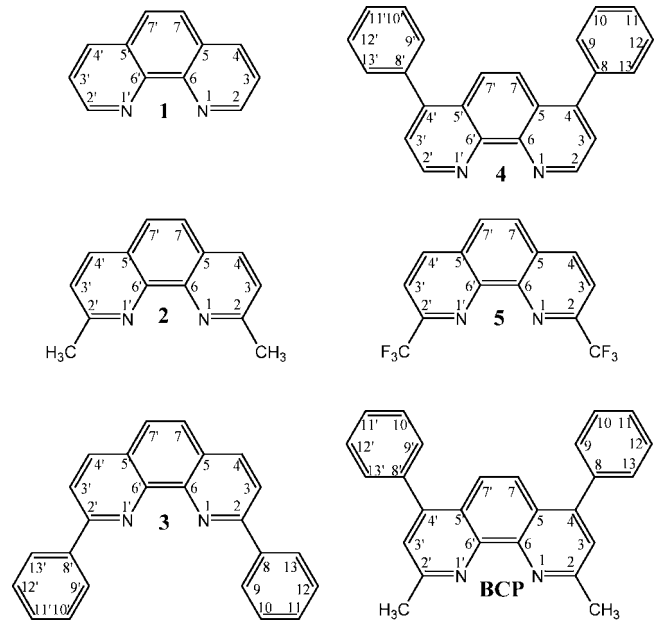


**Figure 2.** Molecular structures of all of the calculated compounds.

The reorganization energy $\lambda$ corresponds to the sum of geometry relaxation energies upon going from the neutral-state geometry to the charged-state geometry and vice versa. Hence, $\lambda$ for electron transfer is given by

$$\lambda = [E^-(g^0) - E^-(g^-)] + [E^0(g^-) - E^0(g^0)] \quad (6)$$

Here, $E^-(g^0)$ and $E^0(g^0)$ are the energies of the anion and neutral state with the optimized geometry of the neutral molecule, respectively; $E^-(g^-)$ and $E^0(g^-)$ are the energies of the anion and neutral states with the optimized anion geometry, respectively.

All of the neutral geometry optimizations were performed at the density functional theory level with the B3LYP function and HF using the Gaussian 03 program suite,[13] involving the gradient correction of the exchange functional by Becke[14] and the correction functional by Lee, Yang, and Parr.[15] $C_2$ symmetry was adopted for all of the compounds. The cation and anion states were optimized based on an unrestricted B3LYP functional, and spin contamination in the radical species was found to be very small ($\langle S^2 \rangle \leqslant 0.76$). The single-excitation configuration interaction (CIS) method was employed to obtain first singlet excited-state structures. The absorption and emission energies were systematically investigated by time-dependent density functional theory (TD-DFT). The charge-transfer integral calculations were performed using the PW91PW91/6-31G* method. It has been demonstrated that this is an appropriate choice of functional for the DFT level.[9b,11a]

## Results and Discussion

**Ground- and Excited-Singlet State Geometries.** The chemical structures of **BCP** and its analogues **1**−**5** are shown in Figure 2. The basic framework of these compounds is the phenanthroline unit, which has an aromatic $\pi$-conjugated backbone and includes two nitrogen atoms in the 1 and 1′ positions of the phenanthroline unit. Generally, the molecular geometry will change upon varying from the ground state to excited states. To understand the relationship between the molecular structure and photophysical properties of **BCP** and its analogues, the geometries of the ground state ($S_0$) and excited singlet state ($S_1$) of the **BCP** and **1**−**5** were investigated. Table 1 summarizes the optimized bond lengths of the $S_0$ and $S_1$ states of **BCP**. The

**TABLE 1: Selected Bond Lengths of BCP in the Ground State ($S_0$) and the Excited State ($S_1$)**

| bond length (Å) | ground state B3LYP/ 6-31G* | ground state HF/ 6-31G* | excited state CIS/ 6-31G* | $R_{CIS} - R_{HF}$ | $(R_{CIS} - R_{HF}) \div R_{HF} \times 100\%$ |
|---|---|---|---|---|---|
| N1−C2 | 1.32416 | 1.29790 | 1.34136 | 0.04346 | 3.34849 |
| N1−C6 | 1.35373 | 1.34358 | 1.30116 | −0.04242 | −3.15724 |
| C2−C3 | 1.41432 | 1.41426 | 1.38876 | −0.02550 | −1.80306 |
| C3−C4 | 1.38377 | 1.36420 | 1.38323 | 0.01903 | 1.39496 |
| C4−C5 | 1.42974 | 1.42359 | 1.44065 | 0.01706 | 1.19838 |
| C5−C6 | 1.42453 | 1.39905 | 1.44504 | 0.04599 | 3.28723 |
| C6−C6′ | 1.46034 | 1.45897 | 1.48604 | 0.02707 | 1.85542 |
| C5−C7 | 1.43273 | 1.43753 | 1.38660 | −0.05093 | −3.54288 |
| C7−C7′ | 1.36326 | 1.34239 | 1.41334 | 0.07095 | 5.28535 |
| C4−C8 | 1.48976 | 1.49576 | 1.47884 | −0.01692 | −1.13120 |
| C2−C($CH_3$) | 1.50963 | 1.50770 | 1.50079 | −0.00691 | −0.45831 |
| C8−C9 | 1.40403 | 1.39023 | 1.39739 | 0.00716 | 0.51502 |
| C9−C10 | 1.39479 | 1.38609 | 1.38325 | −0.00284 | −0.20489 |
| C10−C11 | 1.39574 | 1.38444 | 1.38593 | 0.00149 | 0.10762 |
| C11−C12 | 1.39627 | 1.38624 | 1.38699 | 0.00075 | 0.05410 |
| C12−C13 | 1.39468 | 1.38436 | 1.38244 | −0.00192 | −0.13869 |
| C8−C13 | 1.40486 | 1.39215 | 1.39848 | 0.00633 | 0.45469 |

$R_{CIS} - R_{HF}$ is the difference between the ground-state and excited-state bond distances. The $S_0$ geometry of **BCP** and its analogues is in good agreement with the experimental results determined by the single-crystal X-ray diffraction.[16,17] For the ground state, two methods (HF/6-31G* and B3LYP/6-31G*) were employed to optimize the geometry, which gave similar results. The maximal difference between the corresponding bond lengths obtained by the two methods is 0.026 Å (see Table 1). The comparison between the excited- and ground-state geometries indicates that the molecular structure change is predominantly localized on the phenanthroline moiety and the C4−C8 bond, which links phenanthroline and the phenyl groups. Especially, the central phenyl ring of the phenantroline unit and the C−N bond distances (namely, C6−C5, C5−C7, C6−C6′, C7−C7′, N1−C6, and N1−C2) change evidently. The methyl groups nearly remain unchanged. For the **BCP** analogues **1**, **2**, and **4**, the structure changes take place mainly on the phenanthroline and phenyl group upon these molecules alternating from the ground state to excited state (see Supporting Information). In the excited state, **BCP** and **4** have very similar molecular geometries; for example, the dihedral angles between the phenanthroline plane and the substituted phenyl ring are 47.3° for **4** and 47.9° for **BCP** (Figure 3). These results suggest that the methyl group has little effect on the molecular geometry and that compound **4** may possess similar physical properties to **BCP**. For the excited molecule **3** with two phenyl groups attached at the 2 and 2′ positions of the phenanthroline unit, the dihedral angle between the phenanthroline plane and phenyl ring is 0.3°, which is much smaller than that for **BCP** or **4**. In **3**, the coplanar and conjugated degrees between the phenanthroline plane and two phenyl rings is stronger than that of **BCP**. The geometry optimization result shows that the intramolecular hydrogen bonding interaction between the N atom and the hydrogen atom located on the phenyl ring may exist in molecule **3** (Figure 3), which could make molecule **3** more coplanar. For molecule **5**, two electron withdrawing groups, $CF_3$, are introduced on the positions 2 and 2′ of the phenanthroline moiety. The calculated result demonstrated that the $CF_3$ groups have little effect on the molecular geometries of the phenanthroline moiety in the ground and excited states (see Support Information). However, they have remarkable influence on the frontier molecular orbital energies. All of the calculations indicate that the structural changes for the excited states are mainly located in the phenanthroline moiety.

**Molecular Orbitals, Excitation Energy, and Emission Energy.** The absorption, emission characteristics, and frontier molecular orbitals (FMOs) studies for **BCP** and its analogues (**1**−**5**) have been performed based on the optimized geometries of the $S_0$ and $S_1$ states. The absorption and emission wavelengths were calculated using TD-B3LYP. For **BCP**, the FMO distribution of the $S_0$ state is shown in Figure 4, which is primarily dominated by the orbitals originating from the phenanthroline moiety and phenyl groups. The HOMO is mainly localized on the phenanthroline moiety, which is a large conjugate $\pi$-electron system. The $HOMO_{-1}$ is mainly composed of the orbitals of two nitrogen atoms (Table 2), and the overlap population between the nitrogen atom and neighboring carbon atoms in the $HOMO_{-1}$ orbital is near zero (0.009 and 0.041), indicating that there is no bonding interaction between the nitrogen atom and its adjacent carbon atoms in the $HOMO_{-1}$ orbital. Therefore, $HOMO_{-1}$ is a nonbonding orbital.[18] The $HOMO_{-2}$ comes from the phenanthroline moiety, and $HOMO_{-3}$ and $HOMO_{-4}$ are predominantly located at the phenanthroline moiety and the two phenyl groups. The contributions of p orbitals to $HOMO_{-3}$ and $HOMO_{-4}$ are small; therefore, they are $\sigma$ bonds. Moreover, the LUMO and $LUMO_{+1}$ mainly arise from the phenanthroline and are mainly composed of p orbitals, suggesting that they are $\pi^*$ orbitals.

Compound **4** may be a good hole/exciton-blocking material since its orbital characteric is very similar to that of **BCP**. Interestingly, compound **3** has larger delocalization than **BCP**, which is consistent with the geometry optimization results and may facilitate the charge transfer. For compound **5**, the $CF_3$ groups are not involved in the formation of frontier molecular orbitals but make the occupied orbitals deeper and improve the ionization energy. Therefore, **5** may be suitable for a hole/exciton-blocking material from the molecular design point of view.

Table 3 presents the calculated absorption and emission wavelengths, oscillator strength, and major contribution of **BCP** using TD-B3LYP with 6−31G* basis sets and experimental data. The absorption and the emission wavelengths are predicted at 277.21 and 368.37 nm, respectively. On the basis of population analysis, the absorption is due to the $\pi \rightarrow \pi^*$ ($HOMO_{-2} \rightarrow$ LUMO 24%) and $\sigma \rightarrow \pi^*$ ($HOMO_{-3} \rightarrow$ LUMO 17%, $HOMO_{-4} \rightarrow$ LUMO 19%) electron transitions. This absorption peak shows a moderate oscillator strength ($f$ = 0.0836) due to the effective spatial overlap between FMOs. The $n \rightarrow \pi^*$ ($HOMO_{-1} \rightarrow$ LUMO) and $\pi \rightarrow \pi^*$ (HOMO → LUMO) absorptions are at 306 and 314 nm and have larger oscillator strengths. The $f$ value of the emission is 0.5193. As a result, the emission arises from the transition between the LUMO and HOMO (73%). The electron transitions are mainly located in the phenanthroline moiety.

**Energy Gap.** The computed $S_0 \rightarrow T_1$ excitation energies (energy gap, $E_{T1}$) and the energy difference between the HOMO and LUMO ($\Delta E$) for **BCP** and **1**−**5** based on B3LYP/631G* basis sets are listed in Table 4. The $E_{T1}$, $E_{HOMO}$ (the energy of the HOMO), and $E_{LUMO}$ (the energy of the LUMO) of **BCP** are in agreement with the reported calculations[19] and experimental[20] results. Distinguishing the properties of some hole/exciton-blocking materials with the aid of DFT caculations may be an efficient approach. In principle, if a compound has higher $S_0 \rightarrow T_1$ excitation energy and a deeper LUMO level than **BCP**, it may be a better hole/exciton-blocking material than **BCP**. The calculated results show that the calculated $\Delta E$ has the same

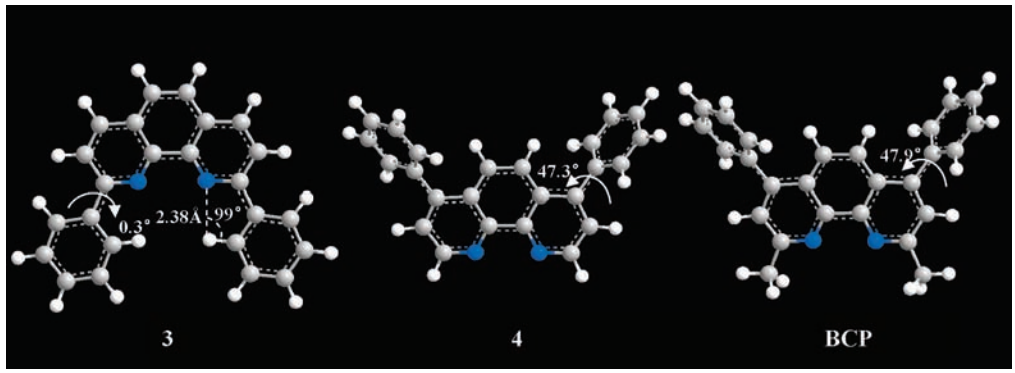


**Figure 3.** Optimized excited singlet-state structures of the compounds **3**, **4**, and **BCP**.

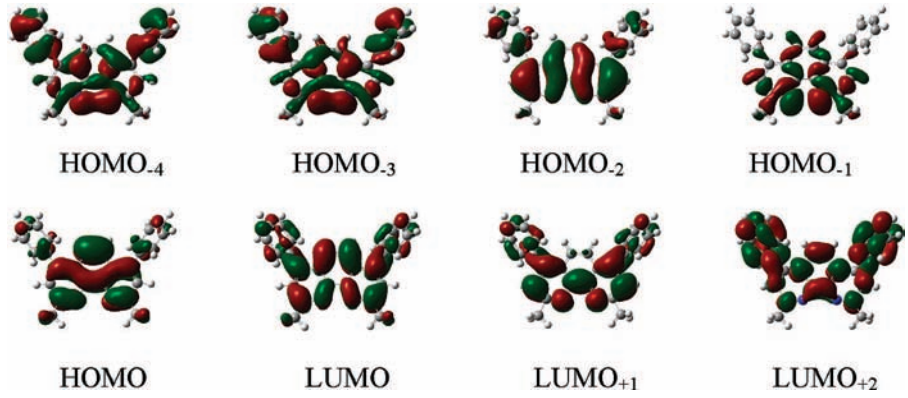


**Figure 4.** Frontier molecular orbitals for the $S_0$ state of the **BCP** molecule.

**TABLE 2: Molecular Orbital Components of BCP (%) (B3LYP/6-31G*)**

| | | phenanthroline | | N atom | | phenyl | | methyl |
|---|---|---|---|---|---|---|---|---|
| no. orbital | orbital energy (eV) | total | p orbital[a] | total | p orbital[a] | total | p orbital[a] | |
| 100($LUMO_{+4}$) | −0.15 | 2.9 | 1.3 | 0.1 | 0.1 | 97.0 | 23.8 | 0.0 |
| 99($LUMO_{+3}$) | −0.29 | 23.5 | 21.1 | 0.4 | 0.3 | 75.6 | 20.6 | 0.9 |
| 98($LUMO_{+2}$) | −0.33 | 50.2 | 47.0 | 0.7 | 0.5 | 48.4 | 13.2 | 1.4 |
| 97($LUMO_{+1}$) | −1.25 | 85.5 | 82.0 | 20.2 | 19.8 | 14.3 | 2.9 | 0.2 |
| 96(LUMO) | −1.28 | 83.8 | 80.6 | 8.3 | 8.0 | 14.2 | 2.9 | 2.0 |
| 95(HOMO) | −5.78 | 87.7 | 83.8 | 10.4 | 9.3 | 9.6 | 2.1 | 2.6 |
| 94($HOMO_{-1}$) | −6.23 | 93.6 | 3.1 | 66.8 | 0.5 | 2.0 | 0.4 | 4.5 |
| 93($HOMO_{-2}$) | −6.28 | 86.2 | 83.7 | 7.7 | 7.4 | 12.4 | 3.0 | 1.3 |
| 92($HOMO_{-3}$) | −6.73 | 61.7 | 14.5 | 33.5 | 1.2 | 35.9 | 9.5 | 2.4 |
| 91($HOMO_{-4}$) | −6.79 | 65.8 | 15.3 | 35.2 | 1.5 | 32.7 | 9.0 | 1.5 |

[a] The p orbital means that the orbital is vertical to the plane in which the molecule resides.

**TABLE 3: Calculated Absorption and Emission Energies, Oscillators Strengths (*f*), the Major Contribution, And Experimental Data of BCP**

| | experiment[6] | calculation | *f* | major contribution |
|---|---|---|---|---|
| absorption | 4.43 eV | 4.47 eV | 0.0836 | $HOMO_{-4} \rightarrow LUMO$ (19%)<br>$HOMO_{-3} \rightarrow LUMO$ (17%)<br>$HOMO_{-2} \rightarrow LUMO$ (24%) |
| absorption | | 3.94 eV | 0.1358 | $HOMO_{-1} \rightarrow LUMO$ (44%)<br>$HOMO \rightarrow LUMO$ (43%) |
| absorption | | 4.05 eV | 0.1630 | $HOMO_{-1} \rightarrow LUMO$ (43%)<br>$HOMO \rightarrow LUMO$ (40%) |
| emission | 3.20 eV | 3.36 eV | 0.5193 | $HOMO_{-2} \rightarrow LUMO_{+2}$ (13%)<br>$HOMO_{-1} \rightarrow LUMO$ (14%)<br>$HOMO \rightarrow LUMO$ (73%) |

change tendency as that of $E_{T1}$, suggesting that $E_{T1}$ could be adjusted by controlling the level of the HOMO and LUMO. The results indicate that the compounds **1** and **2** and **4** and **5** have the potential to be hole/exciton-blocking materials.

**Hole Blocking and Electron Injection.** Additional information derived from the calculations could show the relationship between structure and electronic behavior, in particular, the response of the molecule to the formation of a hole or the addition of an electron. Table 4 summarizes the calculated ionization potentials (IPs) and electron affinities (EAs). It is worth noting that both the vertical and adiabatic IPs or EAs have been calculated. For the calculations of vertical IPs or EAs, only the neutral molecular geometry has been optimized, while for the calculations of adiabatic IPs or EAs, both the neutral and charged molecular geometries have been optimized. For **BCP**, the energy required to create a hole is about 7 eV, while that to inject an electron requires −0.2 eV, which leads to facile electron injection. The experimental IP values are easily obtained,[21] while measuring the electron affinity (the binding energy of the injected electron) is very difficult due to the presence of strong excitonic effects.[22] Therefore, the above calculations provide an appropriate way to estimate the electron affinity. By comparison, it was found that the compounds **1**, **4**, and **5** have higher ionization energies and deeper energies of the LUMO, suggesting that they might be the effective hole-blocking materials.

**TABLE 4: Ionization Potentials, Electron Affinities, and Triplet Energy Levels ($E_{T1}$) (unit: eV) for Compounds 1−5 and BCP**

| series | IP(v)[a] | IP(a)[b] | EA(v)[c] | EA(a)[d] | $E_{HOMO}$ | $E_{LUMO}$ | $\Delta E$[e] | $E_{T1}$ |
|---|---|---|---|---|---|---|---|---|
| **BCP** | 7.15 | 6.96 | 0.02 | −0.22 | −5.78 | −1.28 | 4.50 | 2.74 |
| **1** | 7.99 | 7.85 | 0.27 | 0.12 | −6.25 | −1.41 | 4.84 | 2.84 |
| **2** | 7.63 | 7.47 | 0.40 | 0.22 | −5.99 | −1.20 | 4.79 | 2.84 |
| **3** | 7.01 | 6.90 | −0.38 | −0.51 | −5.72 | −1.69 | 4.04 | 2.52 |
| **4** | 7.36 | 7.19 | −0.10 | −0.30 | −5.97 | −1.46 | 4.51 | 2.72 |
| **5** | 8.54 | 8.38 | −0.57 | −0.78 | −6.87 | −2.18 | 4.69 | 2.77 |

[a] IP(v) = vertical ionization potentials. [b] IP(a) = adiabatic ionization potentials. [c] EA(v) = vertical electron affinities. [d] EA(a) = adiabatic electron affinities. [e] $\Delta E = E_{LUMO} - E_{LUMO}$.

**TABLE 5: Calculated Transport Characteristics of BCP and 1−5**

| compound | reorganization energy $\lambda$(eV) | pathway | dimer CM distance (Å) | transfer integral, $\beta/10^{-4}$eV | diffusion coefficient, $D$(cm$^2$/s) | drift mobility, $\mu$(cm$^2$/V s) |
|---|---|---|---|---|---|---|
| **BCP** | 0.463 | I | 7.098 | 458.280 | 0.00046 | 0.0179 |
| | | II | 12.888 | 90.554 | | |
| **1** | 0.287 | I | 6.903 | 91.156 | 0.00089 | 0.0345 |
| | | II | 4.819 | 326.590 | | |
| | | III | 6.222 | 91.954 | | |
| | | IV | 7.051 | 34.804 | | |
| | | V | 7.570 | 257.712 | | |
| **2** | 0.327 | I | 7.574 | 83.903 | 0.00066 | 0.0256 |
| | | II | 6.500 | 36.594 | | |
| | | III | 7.548 | 5.933 | | |
| | | IV | 6.584 | 121.311 | | |
| | | V | 9.740 | 6.798 | | |
| **3** | 0.252 | I | 10.592 | 35.939 | 0.00892 | 0.3450 |
| | | II | 4.356 | 987.739 | | |
| | | III | 8.832 | 73.403 | | |
| **4** | 0.402 | I | 7.364 | 126.518 | 0.00075 | 0.0290 |
| | | II | 11.175 | 7.074 | | |
| | | III | 6.328 | 469.085 | | |
| **5** | 0.410 | I | 9.933 | 2.305 | 0.00036 | 0.0140 |
| | | II | 9.537 | 0.372 | | |
| | | III | 9.981 | 4.247 | | |
| | | IV | 4.665 | 44.693 | | |
| | | V | 9.537 | 7.339 | | |

**Electron Transport.** The reorganization energies ($\lambda$) computed for all of the compounds are listed in Table 5. All of the results indicate that the reorganization energies depend on not only geometry relaxation but also substituted groups. For instance, upon varying from the neutral to negatively charged state, the alterations of the N1−C6−C6′−N1′ dihedral angle are 6.397° for **BCP** and 0.723° for **3**. Therefore, the **BCP** has a larger reorganization energy. Compound **1** has a smaller reorganization energy than compound **2**, which has two $CH_3$ groups. It could be concluded that the inner reorganization energies will become larger when the 4,4′ and 2,2′ positions of the phenanthroline derivatives are substituted by the electron pushing or withdrawing groups. Furthermore, the electron withdrawing could lead to a larger change of the reorganization energy compared with that of the electron pushing groups.

In this study, the molecular dimer models were obtained directly from the corresponding single-crystal X-ray structures.[16,17] Once a transport pathway is defined, the electronic coupling can be calculated through the diabatic model. Equation 5 was used to calculate the transfer integral. All of the hopping pathways for **BCP**, **1**, **3**, and **4** are shown in Figure 5. The diffusion coefficient ($D$) and drift mobility ($\mu$) of electrons in all of the compounds were estimated at 300 K from eqs 2−4 (Table 5). The dimer center mass (CM) distance and transfer integral ($\beta$) are also presented in Table 5.

The transfer integrals $\beta$ for all compounds in all pathways approximately are in the range of $10^{-4}-10^{-2}$ eV (Table 5). The magnitudes of $\beta$ depend on the overlap degree between the LUMOs of the hopping complex. When the dimer center mass (CM) distance is short and there is obvious orbital overlap between two molecules in a dimer, the $\beta$ values will be large, which could be demonstrated in the case of pathway I for **BCP**. It is also revealed that the intermolecular interaction model in the hopping partners have a dramatic effect on the $\beta$ values.

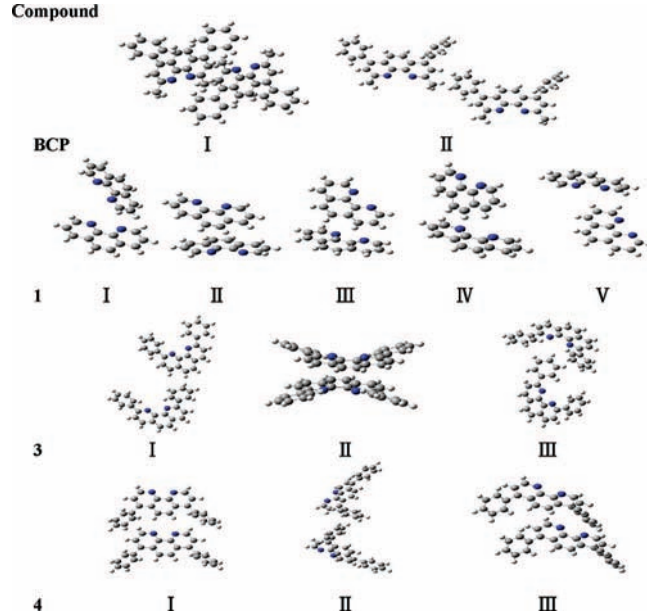


**Figure 5.** All charge-hopping pathways for compounds **BCP**, **1**, **3**, and **4**.

For the pathway II model of compound **3**, two molecules are parallel to each other, and there is a strong intermolecular $\pi-\pi$ interaction resulting in the largest $\beta$(e) value. The calculated electron carrier mobility of **BCP** is comparable with the experimental results of $1.1 \times 10^{-3}$ cm$^2$/(V s), indicating that the calculation results are acceptable.[21] All of the analogues except compound **3** have the approximate electron mobility because they have similar molecular fragments. Compound **3** has the largest electron carrier mobility due to the fact that it has the largest $\beta$ value and the smallest reorganization energy, which could be attributed to its largest conjugated degree between the phenanthroline plane and two phenyl rings. Hopefully, the experimental electron mobility of **BCP** and its analogues may be improved based on the careful optimization of the film formation process. On the basis of the calculations, **BCP** and **1**−**5** are efficient electron-transfer materials compared with a typical electron mobility with a magnitude of $10^{-5}$.[21]

## Conclusions

The equilibrium geometries of the neutral, cationic, and anionic states for all six compounds were optimized by means of the B3LYP and HF methods (only neutral geometries) at the 6-31G* basis sets. The molecular structures of the first singlet excited state were optimized with the CIS method. The absorption and emission energies have been calculated with the TD-DFT method at the optimized geometries. The calculated energies are in good agreement with the experimental values, suggesting that the optimized geometries are reliable. The orbital patterns revealed that the absorption and emission transitions could be attributed to the charge transfer between phenanthroline and phenyl groups or the intraphenanthroline moiety charge transfer. The $S_0 \rightarrow T_1$ excitation energies (energy gap, $E_{T1}$) could be controlled by manipulating the energy level of the HOMO and LUMO. The energy level of the LUMO would be adjusted by modifying the molecular structures.

To introduce phenyl groups on the 2,2′ positions of phenanthroline could lead to the decrease of the $\lambda$ (the reorganization energy) value, while neither the addition of electron pushing groups nor electron withdrawing groups on the 2,2′ or 4,4′ positions of phenanthroline would result in the increase of the $\lambda$ value. The dimer center mass (CM) distance and the intermolecular contact model in the hopping partners have a dramatic effect on the $\beta$ values. The drift mobility calculation results demonstrated that all compounds **BCP** and **1**−**5** studied in this paper are efficient electron-transfer materials. Furthermore, compounds **1**, **4**, and **5** may be efficient hole/exciton-blocking materials compared with compounds **3** and **2**.

**Acknowledgment.** The authors thank Prof. Shuai Z. and Mrs. Yang X. for discussing the direct method of calculating the charge-transfer integral and acknowledge the financial support from the Supported by Program for Changjiang Scholars and Innovative Research Team in University, the National Natural Science Foundation of China (20373009, 20573016, and 50733002), and the Major State Basic Research Development Program (2002CB613401).

**Supporting Information Available:** Tables of selected bond lengths in the ground and excited singlet state for compounds **1**−**5** (**S1**−**S5**) and tables of molecular orbital components for compounds **1**−**5** (**S6**−**S10**). Figures of frontier molecular orbitals for the ground state of all of the compounds (Figure S1) and charge-hopping pathways for compounds **2** and **5** (Figure S2). This material is available free of charge via the Internet at http://pubs.acs.org.

## References and Notes

(1) (a) Loy, D. E.; Koene, B. E.; Thompson, M. E. *Adv. Funct. Mater.* **2002**, *12*, 245. (b) Tang, C. W.; Vanslyke, S. A. *Appl. Phys. Lett.* **1987**, *51*, 913. (c) Adachi, C.; Tokito, S.; Tsutsui, T.; Saito, S. *Jpn. J. Appl. Phys* **1988**, *27*, L713.

(2) (a) Adachi, C.; Nagai, K.; Tamoto, N. *Appl. Phys. Lett.* **1995**, *66*, 2679. (b) O'Brien, D. F.; Burrows, P. E.; Forrest, S. R.; Koene, B. E.; Loy, D. E.; Thompson, M. E. *Adv. Mater.* **1998**, *10*, 1108. (c) Shirota, Y. *J. Mater. Chem.* **2000**, *10*, 1. (d) Hung, L. S.; Chen, C. H. *Mater. Sci. Eng., R* **2002**, *39*, 143. (e) Hreha, R. D.; George, C. P.; Haldi, A.; Domercq, B.; Malagoli, M.; Barlow, S.; Bredas, J. L.; Kippelen, B.; Marder, S. R. *Adv. Funct. Mater.* **2003**, *13*, 967. (f) Nomura, M.; Shibasaki, Y.; Ueda, M.; Tugita, K.; Ichikawa, M.; Taniguchi, Y. *Macromolecules* **2004**, *37*, 1204. (g) Yu, G.; Yin, S. W.; Liu, Y. Q.; Chen, J. S.; Xu, X. J.; Sun, X. B.; Ma, D. G.; Zhan, X. W.; Peng, Q.; Shuai, Z. G.; Tang, B. Z.; Zhu, D. B.; Fang, W. H.; Luo, Y. *J. Am. Chem. Soc.* **2005**, *127*, 6335. (h) Liu, M. S.; Niu, Y. H.; Luo, J. D.; Chen, B. Q.; Kim, T. D.; Bardecker, J.; Jen, A. K. Y. *Polym. Rev.* **2006**, *46*, 7. (i) Shirota, Y.; Kageyama, H. *Chem. Rev.* **2007**, *107*, 953.

(3) Adamovich, V. I.; Cordero, S. R.; Djurovich, P. I.; Tamayo, A.; Thompson, M. E.; D'Andrade, B. W.; Forrest, S. R. *Org. Electron.* **2003**, *4*, 77.

(4) (a) Baldo, M. A.; Lamansky, S.; Burrows, P. E.; Thompson, M. E.; Forrest, S. R. *Appl. Phys. Lett.* **1999**, *75*, 4. (b) Adachi, C.; Baldo, M. A.; Forrest, S. R.; Thompson, M. E. *Appl. Phys. Lett.* **2000**, *77*, 904. (c) Lamansky, S.; Djurovich, P.; Murphy, D.; Abdel-Razzaq, F.; Lee, H. E.; Adachi, C.; Burrows, P. E.; Forrest, S. R.; Thompson, M. E. *J. Am. Chem. Soc.* **2001**, *123*, 4304.

(5) (a) Hill, I. G.; Kahn, A. *J. Appl. Phys.* **1999**, *86*, 4515. (b) Hill, I. G.; Milliron, D.; Schwartz, J.; Kahn, A. *Appl. Surf. Sci.* **2000**, *166*, 354. (c) Yang, J. H.; Gordon, K. C. *Chem. Phys. Lett.* **2003**, *375*, 649. (d) Ben Khalifa, M.; Vaufrey, D.; Tardy, J. *Org. Electron.* **2004**, *5*, 187. (e) Kim, Y.; Im, W. B. *Phys. Status Solidi A* **2004**, *201*, 2148. (f) Yoon, Y. B.; Yang, H. W.; Choo, D. C.; Kim, T. W.; Oh, H. S. *Solid State Commun.* **2005**, *134*, 367. (g) Wang, Y. M.; Teng, F.; Zhou, Q. C.; Wang, Y. S. *Appl. Surf. Sci.* **2006**, *252*, 2355.

(6) Tang, H. Q.; Liao, H. X.; Zhu, L. H. *Chem. Phys. Lett.* **2003**, *381*, 605.

(7) (a) Coropceanu, V.; Cornil, J.; da Silva, D. A.; Olivier, Y.; Silbey, R.; Bredas, J. L. *Chem. Rev.* **2007**, *107*, 926. (b) Bredas, J. L.; Beljonne, D.; Coropceanu, V.; Cornil, J. *Chem. Rev.* **2004**, *104*, 4971. (c) Nelsen, S. F.; Trieber, D. A.; Ismagilov, R. F.; Teki, Y. *J. Am. Chem. Soc.* **2001**, *123*, 5684. (d) Nelsen, S. F.; Blomgren, F. *J. Org. Chem.* **2001**, *66*, 6551. (e) Sakanoue, K.; Motoda, M.; Sugimoto, M.; Sakaki, S. *J. Phys. Chem. A* **1999**, *103*, 5551. (f) Malagoli, M.; Bredas, J. L. *Chem. Phys. Lett.* **2000**, *327*, 13. (g) Li, X. Y.; Tong, J.; He, F. C. *Chem. Phys.* **2000**, *260*, 283. (h) Marcus, R. A.; Sutin, N. *Biochim. Biophys. Acta* **1985**, *811*, 265.

(8) (a) Marcus, R. A. *Rev. Mod. Phys.* **1993**, *65*, 599. (b) Balzani, V.; Juris, A.; Venturi, M.; Campagna, S.; Serroni, S. *Chem. Rev.* **1996**, *96*, 759.

(9) (a) Deng, W. Q.; Goddard, W. A. *J. Phys. Chem. B* **2004**, *108*, 8614. (b) Song, Y. B.; Di, C. A.; Yang, X. D.; Li, S. P.; Xu, W.; Liu, Y. Q.; Yang, L. M.; Shuai, Z. G.; Zhang, D. Q.; Zhu, D. B. *J. Am. Chem. Soc.* **2006**, *128*, 15940. (c) Schein, L. B.; McGhie, A. R. *Phys. Rev. B* **1979**, *20*, 1631. (d) Yang, X.; Li, Q.; Shuai, Z. *Nanotechnology* **2007**, *18*, 424029. (e) Yang, X.; Wang, L.; Wang, C.; Long, W.; Shuai, Z. *Chem. Mater.* **2008**, *20*, 3205.

(10) (a) Lin, B. C.; Cheng, C. P.; You, Z. Q.; Hsu, C. P. *J. Am. Chem. Soc.* **2005**, *127*, 66. (b) Hutchison, G. R.; Ratner, M. A.; Marks, T. J. *J. Am. Chem. Soc.* **2005**, *127*, 16866. (c) Cornil, J.; Beljonne, D.; Calbert, J. P.; Brédas, J. L. *Adv. Mater.* **2001**, *13*, 1053.

(11) (a) Troisi, A.; Orlandi, G. *Chem. Phys. Lett.* **2001**, *344*, 509. (b) Yin, S. W.; Yi, Y. P.; Li, Q. X.; Yu, G.; Liu, Y. Q.; Shuai, Z. G. *J. Phys. Chem. A* **2006**, *110*, 7138.

(12) (a) Valeev, E. F.; Coropceanu, V.; da Silva Filho, D. A.; Salman, S.; Brédas, J. L. *J. Am. Chem. Soc.* **2006**, *128*, 9882. (b) Grzegorczyk, W. J.; Savenije, T. J.; Valeton, J. J. P.; Fratiloiu, S.; Grozema, F. C.; de Leeuw, D. M.; Siebbeles, L. D. A. *J. Phys. Chem. C* **2007**, *111*, 18411. (c) Prins, P.; Senthilkumar, K.; Grozema, F. C.; Jonkheijm, P.; Schenning, A. P. H. J.; Meijer, E. W.; Siebbeles, L. D. A. *J. Phys. Chem. B* **2005**, *109*, 18267.

(13) Frisch, M. J.; Trucks, G. W.; Schlegel, H. B.; Scuseria, G. E.; Robb, M. A.; Cheeseman, J. R.; Montgomery, J. A., Jr.; Vreven, T.; Kudin, K. N.; Burant, J. C.; Millam, J. M.; Iyengar, S. S.; Tomasi, J.; Barone, V.; Mennucci, B.; Cossi, M.; Scalmani, G.; Rega, N.; Petersson, G. A.; Nakatsuji, H.; Hada, M.; Ehara, M.; Toyota, K.; Fukuda, R.; Hasegawa, J.; Ishida, M.; Nakajima, T.; Honda, Y.; Kitao, O.; Nakai, H.; Klene, M.; Li, X.; Knox, J. E.; Hratchian, H. P.; Cross, J. B.; Adamo, C.; Jaramillo, J.; Gomperts, R.; Stratmann, R. E.; Yazyev, O.; Austin, A. J.; Cammi, R.; Pomelli, C.; Ochterski, J. W.; Ayala, P. Y.; Morokuma, K.; Voth, G. A.; Salvador, P.; Dannenberg, J. J.; Zakrzewski, V. G.; Dapprich, S.; Daniels, A. D.; Strain, M. C.; Farkas, O.; Malick, D. K.; Rabuck, A. D.; Raghavachari, K.; Foresman, J. B.; Ortiz, J. V.; Cui, Q.; Baboul, A. G.; Clifford, S.; Cioslowski, J.; Stefanov, B. B.; Liu, G.; Liashenko, A.; Piskorz,

P.; Komaromi, I.; Martin, R. L.; Fox, D. J.; Keith, T.; Al-Laham, M. A.; Peng, C. Y.; Nanayakkara, A.; Challacombe, M.; Gill, P. M. W.; Johnson, B.; Chen, W.; Wong, M. W.; Gonzalez, C.; Pople, J. A. *Gaussian 03*, Revision C.02; Gaussian, Inc.: Pittsburgh, PA, 2003.

(14) (a) Becke, A. D. *Phys. Rev. A* **1988**, *38*, 3098. (b) Becke, A. D. *J. Chem. Phys.* **1993**, *98*, 1372.

(15) Lee, C.; Yang, W.; Parr, R. G. *Phys. Rev. B* **1988**, *37*, 785.

(16) (a) Nishigaki, S.; Yoshioka, H.; Nakatsu, K. *Acta Crystallogr., Sect. B* **1978**, *34*, 875. (b) Bailey, P.; Parsons, S.; Messenger, D.; Dick, C. 2005,Private Communication. (c) Gembicky, M.; Kovalevsky, Yu. A.; Coppens, P. 2004,Private Communication. (d) Ceolin, R.; Mariaud, M.; Levillain, P.; Rodier, N. *Acta Crystallogr., Sect. B* **1979**, *35*, 1630. (e) Kovalevsky, Yu. A.; Gembicky, M.; Coppens, P. 2003,Private Communication.

(17) Wang, J.; Ye, J. W.; Ye, L.; Yu, D. Y.; Wang, Y. *Acta Crystallogr., Sect. E* **2007**, *63*, o2007.

(18) (a) Haslingerova, I. *Czech. J. Phys.* **1977**, *27*, 1389. (b) Glassey, W. V.; Hoffmann, R. *J. Chem. Phys.* **2000**, *113*, 1698.

(19) Marsal, P.; Avilov, I.; da Silva, D. A.; Bredas, J. L.; Beljonne, D. *Chem. Phys. Lett.* **2004**, *392*, 521.

(20) Baldo, M. A.; Forrest, S. R. *Phys. Rev. B* **2000**, *62*, 10958.

(21) Kulkarni, A. P.; Tonzola, C. J.; Babel, A.; Jenekhe, S. A. *Chem. Mater.* **2004**, *16*, 4556.

(22) Schmidt, A.; Anderson, M. L.; Armstrong, N. R. *J. Appl. Phys.* **1995**, *78*, 5619.

JP804308E